Proc. 2nd Japan-China Joint Workshop on Positron Science
JJAP Conf. Proc. **2** (2014) 011205

Comparison Study of Mesoporous Thin Films Characterized by Low-energy Positron Lifetime Spectroscopy and Flow-type Ellipsometric Porosimetry

Shigeru Yoshimoto[1,*], Kenji Ito[2,*], Hiroyuki Hosomi[1], and Yoshihiro Takai[1]

[1] *Toray Research Center, Inc., Otsu, Shiga 520–8567, Japan*
[2] *National Institute of Advanced Industrial Science and Technology (AIST), Tsukuba, Ibaraki 305–8565, Japan*

E-mail: Shigeru_Yoshimoto@trc.toray.co.jp, k-ito@aist.go.jp

(Received May 29, 2014)

Flow-type ellipsometric porosimetry (EP) and low-energy positron annihilation lifetime spectroscopy (PALS) were applied to the pore characterization for two types of nanoporous methyl silsesquioxane thin films fabricated on silicon wafers, in order to examine the consistency between the porosities characterized by both techniques. The sizes of the mesopores in the films were evaluated from the respective pore size distributions, obtained using flow-type EP from *n*-hexane adsorption isotherms at 26 °C based on the Barrett-Joyner-Halenda (BJH) model, while the longest-lived *ortho*-positronium (*o*-Ps) lifetimes for the films were measured using low-energy PALS at an incident positron energy of 1.5 keV. The relationship between the pore size and the *o*-Ps lifetime is discussed in comparison with previously reported measurements for various porous substances.

1. Introduction

In order to improve the target functionality of various thin films, such as low-k interlayer dielectrics and ion separation membranes, much effort has been directed towards controlling the nanoporosity of such films in the nanotechnology industry. Reliable evaluation of the engineered porosity with high sensitivity is therefore a key issue in the development of innovative materials with the desired nanopore characteristics. In the characterization of the nanoscaled pores of thin films, only a small sample quantity, typically sub-micro grams, is generally available for the analysis. In addition to this, it is necessary to examine the sub-micrometers-thick film fabricated on a substrate as is.

Ellipsometric porosimetry (EP) [1] and low-energy positron annihilation lifetime spectroscopy (PALS) [2] are well documented as sensitive tools for evaluating the mesoporosity of thin films on substrates. However, the consistency between the porosities obtained by both techniques has not been quite established. In this study, we applied flow-type EP to the elucidation of the pore size distribution for nanoporous methyl silsesquioxane (MSSQ) backboned thin films fabricated on silicon wafers, in order to compare the mesopore size from flow-type EP with the long-lived *ortho*-positronium (*o*-Ps) lifetimes from PALS. The feasibility of the EP technique for calibrating *o*-Ps lifetime with pore size is discussed in comparison with the data previously reported for various porous substances.

2. Experiments

2.1 Porous films

Two types of MSSQ films with thicknesses of 610 nm (Film A) and 150 nm (Film B) on silicon wafers were examined in the present work. The refractive indices at a wavelength of 630 nm for films A and B were 1.167 and 1.218, respectively. Fourier transform infrared spectroscopy was performed to elucidate the chemical structure of the films, and the obtained spectra are shown in Fig. 1. Pronounced

absorption bands were observed from 1000 cm^{-1} to 1200 cm^{-1} and from 1250 cm^{-1} to 1300 cm^{-1} in the spectra due to the stretching vibration of Si–O and Si–CH_3 bonds, respectively, indicative of the network structure from the methyl-silssquioxane precursor.

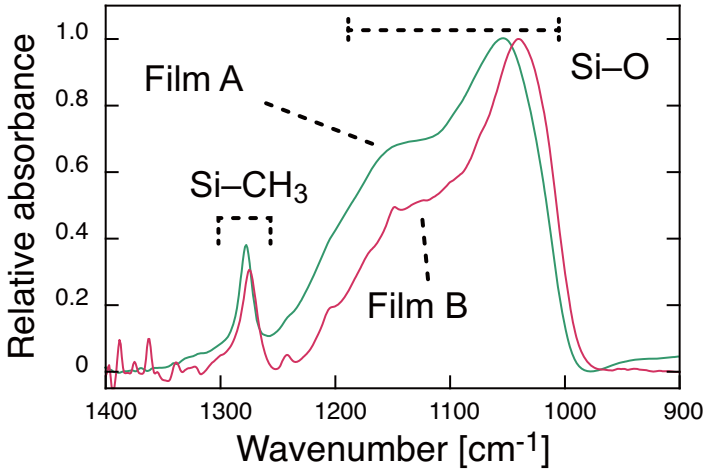

Fig. 1. FT-IR spectra for the present methyl-silsesquioxane backbone films.

2.2 Low-energy positron annihilation lifetime spectroscopy

Positron annihilation lifetime measurements for the films were carried out at $E = 1.5$ keV by utilizing an intense pulsed-positron beam generated with an electron linear accelerator [6]. The measurements were performed at room temperature in vacuum. For each measurement 3 million annihilation event counts were accumulated. To suppress the diffusion of *o*-Ps from the film surface, a nonporous thin film was fabricated on the top of each film sample. A multi-exponential analysis was applied to the recorded lifetime data to deduce the long-lived *o*-Ps lifetime component.

2.3 Ellipsometric porosimetry

Physisorption isotherms of *n*-heptane at 26 °C for the present films were examined using a specially-designed flow-type ellipsometric porosimeter equipped with a sample chamber having a fused-silica optical window and a heat stage. Before the physisorption measurements, the porous film samples were heated at 200 °C under a nitrogen gas flow for ~10 min to remove impurities adsorbed on the pore surface of the films. Ellipsometric parameters (Δ, Ψ) at wavelengths from 300 nm to 800 nm were measured with varying flow rate ratio $f_r = f_s/(f_d+f_s)$ from 0 to 0.95. Here, f_s and f_d represent the flow rates for nitrogen gas saturated by *n*-heptane vapor and a dry nitrogen gas, respectively, and the total flow rate f_d+f_s was fixed to 500 sccm. Hence, f_r is proportional to the relative *n*-heptane concentration divided by the saturated concentration at constant temperature, corresponding to the relative pressure of *n*-heptane to the saturated pressure. The observed (Δ, Ψ) parameters were analyzed based on an ambient-film-substrate three-layer model under the assumption of the Cauchy model [7,8], describing the refractive index n as a function of wavelength λ. In order to obtain the isotherms, the variation of the overall refractive index n_o at $\lambda = 630$ nm upon successive adsorption/desorption of the *n*-heptane adsorbate were elucidated as a function of f_r.

Based on the Lorentz–Lorenz equation, $A\rho = (n^2 - 1)/(n^2 + 2)$ (A is a constant and ρ is the

density), the film porosity V_p is expressed as follows,

$$V_p = 1 - \left(\frac{n_f^2 - 1}{n_f^2 + 2}\right) \Big/ \left(\frac{n_s^2 - 1}{n_s^2 + 2}\right) \quad , \tag{1}$$

where n_f and n_s represent the refractive indices for the film and the silica skeleton, respectively. The specific amounts of heptane molecules adsorbed on the film are assumed to be proportional to the volume fraction occupied by heptane molecules V_f. Based on the mean-field approximation, V_f is evaluated from the following equation,

$$\left(\frac{n_o^2 - 1}{n_o^2 + 2}\right) = V_f\left(\frac{n_a^2 - 1}{n_a^2 + 2}\right) + (V_p - V_f)\left(\frac{n_u^2 - 1}{n_u^2 + 2}\right) + (1 - V_p)\left(\frac{n_s^2 - 1}{n_s^2 + 2}\right) \quad , \tag{2}$$

where n_a and n_u are the refractive indices for the adsorbed heptane and the vacuum (= 1), respectively. By substituting Eq. (1) for V_p, we obtain

$$V_f = \left[\left(\frac{n_o^2 - 1}{n_o^2 + 2}\right) - \left(\frac{n_f^2 - 1}{n_f^2 + 2}\right)\right] \Big/ \left(\frac{n_a^2 - 1}{n_a^2 + 2}\right) \quad . \tag{3}$$

For the present work, n_f and n_a were fixed to the refractive indices for the corresponding films with $f_r = 0$ and for the bulk *n*-heptane (1.386) [3]. By using Eq. (3) with the measured n_o, the physisorption isotherms for the films were obtained as the variation of V_f as a function of f_r.

The pore diameter D_p, filled by the adsorbate at f_r, is evaluated from the Kelvin radius r_k and the layer thickness of the adsorbate t, obtained by the following expressions [4],

$$\begin{aligned} r_k &= 2\frac{\gamma V_L}{RT} \ln(f_r) \quad , \\ t &= -t_m \left[\frac{5}{\log(f_r)}\right] \quad , \end{aligned} \tag{4}$$

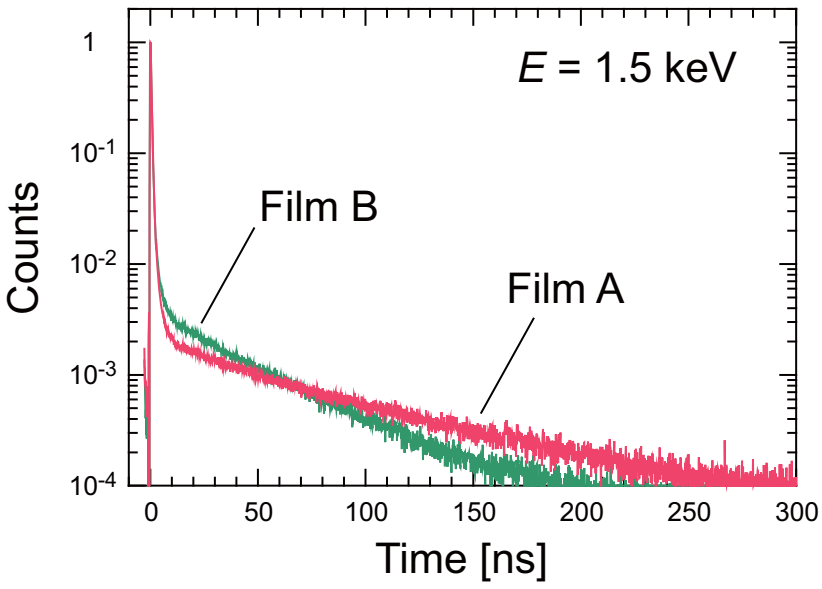

Fig. 2. Normalized positron annihilation lifetime data for the MSSQ porous films. The background signals for the respective data are corrected using the reference data for Kapton.

where γ and V_L represent the surface tension and the occupied molar volume of the adsorbate, R and T are the gas constant and the temperature (= 26 °C), and t_m is the monolayer thickness of the adsorbate [5], estimated by $t_m = M_w/(\rho_a \sigma_a N_0)$, where M_w, ρ_a, and σ_a are the molecular weight, the density, and the cross-sectional area for the adsorbate, respectively. N_0 denotes the Avogadro number and 0.38 nm was adopted for t_m in the present work [5]. Under the assumption that the pores have a cylindrical shape, D_p was estimated as $2(r_k + t)$ for the present films.

3. Results and discussion

Figure 2 shows the positron annihilation lifetime data measured at E = 1.5 keV for films A and B. For both films a long-lived lifetime component due to *o*-Ps annihilation in open spaces is observed. The slope of the *o*-Ps component for film B is significantly steeper than for film A, indicating that the average pore size for film B is smaller than film A. Table 1 lists the results of *o*-Ps lifetimes $\tau^{o\text{-Ps}}$ and their relative intensities $I^{o\text{-Ps}}$, obtained through a least-squares fit to the data. The analysis was performed using three components for the *o*-Ps annihilation lifetime, in which the number of the components was chosen so as to obtain the best fitting parameters. It is known that a $\tau^{o\text{-Ps}}$ longer than 20 ns–30 ns is ascribed to mesopores with a size larger than ~1 nm [9–12], while a $\tau^{o\text{-Ps}}$ shorter than that is attributed to subnanoscale spaces. In particular for the present system, $\tau_1^{o\text{-Ps}}$ and $\tau_2^{o\text{-Ps}}$ may be ascribed to the cage structure in the silica network and micropores, respectively. In the last paragraph of this section, the longest lifetimes $\tau_3^{o\text{-Ps}}$ which are ascribed to mesopores are discussed, in comparison with the mesopore sizes obtained by EP.

Table I. *ortho*-Positronium lifetimes and their relative intensities for the MSSQ porous films.

ID	$\tau_1^{o\text{-Ps}}$ [ns]	$I_1^{o\text{-Ps}}$ [%]	$\tau_2^{o\text{-Ps}}$ [ns]	$I_2^{o\text{-Ps}}$ [%]	$\tau_3^{o\text{-Ps}}$ [ns]	$I_3^{o\text{-Ps}}$ [%]
A	1.59	10.3	20.3	2.6	86.0	17.7
B	1.71	10.8	17.3	3.1	48.3	19.0

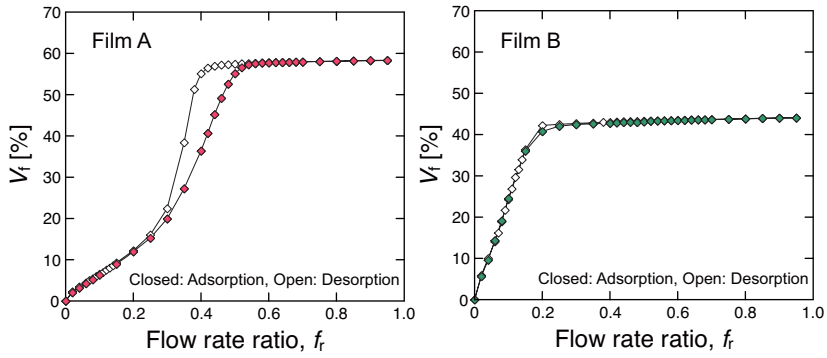

Fig. 3. *n*-Heptane physisorption isotherms at 26 °C observed for the porous films A and B.

Figure 3 shows *n*-heptane physisorption isotherms at 26 °C observed for the porous films A and B as a function of f_r. For film A the adsorption-desorption branches display a hysteresis loop around

f_r = 0.4, ascribed to the type IV isotherm, characteristic of a material containing mesopores [4]. This hysteresis loop is expected to originate from the difference of the meniscus, caused by the capillary condensation of adsorbates in the pores, between the adsorption and desorption processes. This suggests that the necked structure of the mesopores are involved with the physisorption process. On the other hand, the isotherm for the film B shows no hysteresis loop, while V_f increases with increasing f_r from zero to around 0.2. The quantity of adsorption in this region indicates that multiple layers of adsorbates are formed on the mesopore surface. For both the isotherms V_f approaches a constant value with increasing f_r above 0.5, ascribed to the open porosity for the corresponding films, namely, ~60 % for film A and ~45 % for film B, respectively.

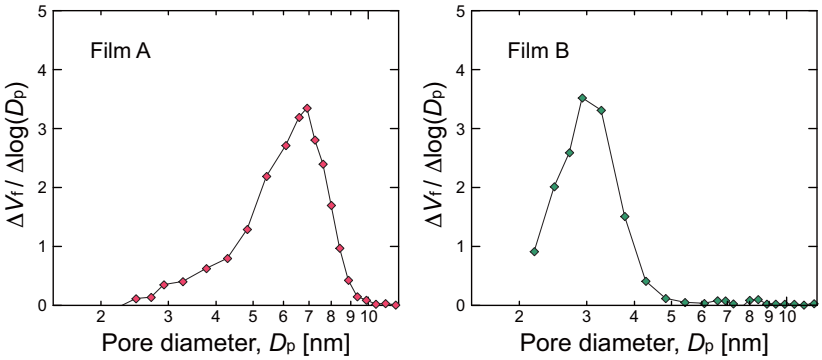

Fig. 4. Pore size distribution (PSD) for the porous films A and B. Each PSD was calculated from the corresponding adsorption branch of Fig. 3.

Figure 4 shows the pore size distribution (PSD) for the porous films A and B, calculated based on the Barrett-Joyner-Halenda (BJH) model [13] from the corresponding adsorption branch of Fig. 3. Pronounced peaks are observed in both PSD, with a maximum at a pore size D_p of ~7 nm and ~3 nm

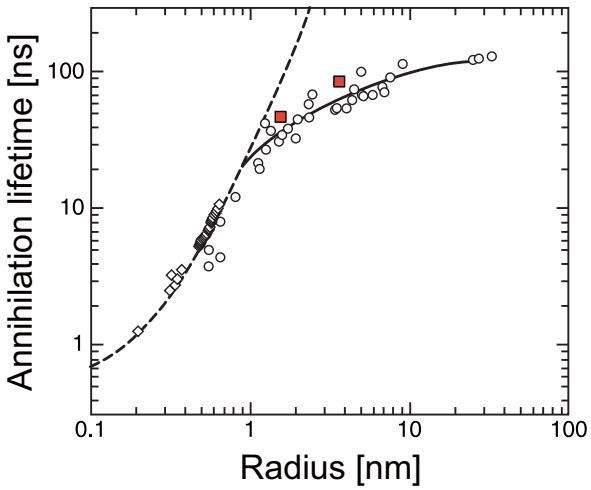

Fig. 5. Relationship between the *o*-Ps lifetime and the pore radius for various substances. The red square symbols represent the data from $\tau_3^{o\text{-Ps}}$ and $D_p/2$ for the films A and B. The data, except those obtained tin the present work, are quoted from Ref. [9], reproduced with permission. Copyright 2014 American Chemical Society.

for films A and B, respectively. This is consistent with the results from PALS which indicate a larger average mesopore size for film A than for films B.

Figure 5 shows the relationship between the measured longest *o*-Ps lifetimes and the mode values of the PSD for the present films, plotted with those for various substances previously reported by our group [9]. The broken and solid lines represent the theoretical correlations for pore size below and above ~1 nm in radius, proposed by Tao and Eldrup [14, 15] and Ito [9], respectively. As seen in this figure, the data for the present films are in rather good agreement with the measurements for the other mesoporous materials (the open circles in the figure), while those data are somewhat scattered. This signifies that the flow-type EP technique is a promising tool for calibrating the *o*-Ps lifetime with the pore size in mesoporous films and can contribute to the development of more sophisticated of models [9–12] connecting the *o*-Ps lifetimes to the exact pore sizes.

4. Summary

Flow-type EP and low-energy PALS have been applied to the pore characterization for two types of MSSQ thin films with different open porosities of ~60 % (film A) and ~45 % (film B). The pore size distributions for the films, obtained from the *n*-hexane adsorption isotherms at 26 °C based on the BJH model, showed that the modal values of the pore diameter are ~7 nm and ~3 nm for the films A and B, respectively. The longest-lived *o*-Ps lifetimes for the respective films were evaluated as ~86 ns and ~46 ns, ascribed to the annihilations in mesopores of the films. The relationship between the obtained pore diameter and the longest-lived *o*-Ps lifetime for the present films displayed a rather good consistency with that obtained previously for various porous substances.

Acknowledgment

The authors express their appreciation to Dr. R. Suzuki and Dr. T. Ohdaira of AIST for their assistance to the positron lifetime measurements.

References

[1] M. R. Baklanov and K. P. Mogilnikov: Microelectron. Eng. **64** (2002) 335.
[2] R. Suzuki: *Positronium in Si and SiO_2 Thin Films* in *Principles and Applications of Positron and Positronium Chemistry* (World Scientific, Singapore, 2003).
[3] Nihonkagakukai-hen, *Kagakubinran Kisohen* (Maruzen, Tokyo, 2004) 5th Ed.
[4] S. J. Gregg and S. W. Sing: *Absorption Surfase and Porosity* (Academic Press, London, 1981) 2nd Ed.
[5] S. Fatemi, M. A. Moosavian, G. Abolhamd, Y. Mortazavi, and R. R. Hudgins: Can. J. Chem. Eng. **80** (2002) 231.
[6] R. Suzuki, Y. Kobayashi, T. Mikado, H. Ohgaki, M. Chiwaki, T. Yamazaki, and T. Tomimasu: Jpn. J. Appl. Phys. Pt. B Lett. **30** (1991) L532.
[7] H. G. Tompkins and W. A. McGahan: *Spectroscopic Ellipsometry and Reflectometry: A User's Guide* (John Wiley & Sons, New York, 1999).
[8] S. Zangooie, R. Bjorklund, and H. Arwin: J. Electrochem. Soc. **144** (1997) 4027.
[9] K. Ito, H. Nakanishi, and Y. Ujihira: J. Phys. Chem. B **103** (1999) 4555.
[10] J. H. Yim, M. R. Baklanov, D. W. Gidley, H. Peng, H. D. Jeong, and L. S. Pu: J. Phys. Chem. B **108** (2004) 26.
[11] T. Goworek, K. Ciesielski, B. Jasinska, and J. Wawryszczuk: Chem. Phys. **230** (1998) 305.
[12] K. Wada and T. Hyodo: J. Phys.-Conf. Ser. **443** (2013) 012003.
[13] E. P. Barrett, L. G. Joyner, and P. H. Halenda: J. Am. Chem. Soc. **73** (1951) 373.
[14] S. J. Tao: J. Chem. Phys. **56** (1972) 5499.
[15] M. Eldrup, D. Lightbody, and J. N. Sherwood: Chem. Phys. **63** (1981) 51.